

# CLiF-VQA: Enhancing Video Quality Assessment by Incorporating High-Level Semantic Information related to Human Feelings

Yachun Mi, Yu Li, Yan Shu, Chen Hui, Puchao Zhou, Shaohui Liu\*  
Harbin Institute of Technology

## Abstract

Video Quality Assessment (VQA) aims to simulate the process of perceiving video quality by the human visual system (HVS). The judgments made by HVS are always influenced by human subjective feelings. However, most of the current VQA research focuses on capturing various distortions in the spatial and temporal domains of videos, while ignoring the impact of human feelings. In this paper, we propose CLiF-VQA, which considers both features related to human feelings and spatial features of videos. In order to effectively extract features related to human feelings from videos, we explore the consistency between CLIP and human feelings in video perception for the first time. Specifically, we design multiple objective and subjective descriptions closely related to human feelings as prompts. Further we propose a novel CLIP-based semantic feature extractor (SFE) which extracts features related to human feelings by sliding over multiple regions of the video frame. In addition, we further capture the low-level-aware features of the video through a spatial feature extraction module. The two different features are then aggregated thereby obtaining the quality score of the video. Extensive experiments show that the proposed CLiF-VQA exhibits excellent performance on several VQA datasets.

## 1. Introduction

With the rapid advancement of technology, the threshold of video production has been significantly lowered, enabling an increasing number of users to create and upload videos to various online platforms (e.g., TikTok, YouTube). However, user-generated content (UGC) videos often have annoying distortion because of the absence of professional filming equipment and skills. Therefore, Video Quality Assessment (VQA) of in-the-wild videos is increasingly important for major video platforms to filter out and enhance low-quality videos.

The lack of raw information and the diversity of con-

\*Corresponding author.

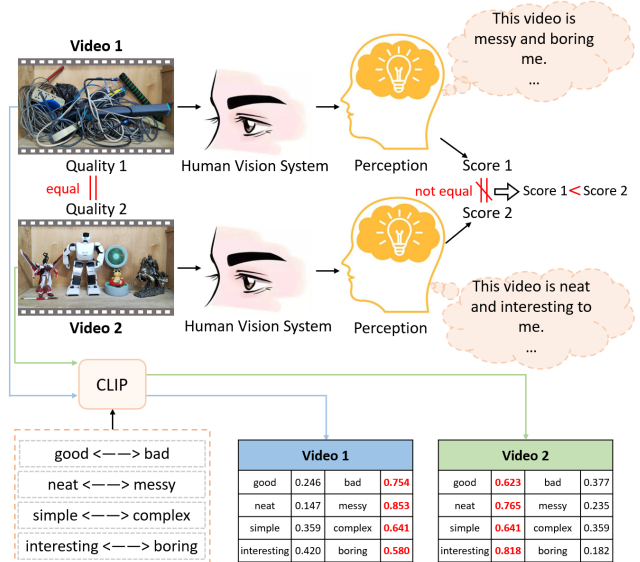


Figure 1. Validating the impact of human feelings on HVS for VQA and the relevance of CLIP with human feelings in video perception. Two videos with the same quality captured in the same scene using the same equipment. CLIP show high consistency with human perception in video perception. We selected 10 subjects to perform VQA on the two videos and took their mean value as the video quality score.

tent and distortion types in in-the-wild videos present a significant challenge for VQA research. Fortunately, there are many subjective experiments that provide high-quality datasets [17, 27, 35, 40, 48, 61], which are labeled according to human mean opinion scores (MOS). With the benefit of these datasets, the current VQA methods can perform supervised training on them to fit the MOS as best as possible. Traditional VQA methods [1, 5, 8, 22, 28, 34, 38, 45] are successful in predicting the quality of perceptual videos, which model spatial and temporal distortions using hand-crafted features. However, the hand-crafted features have a low correlation with human perception, so its outcomes are not always reliable. In recent years, with the advancement of deep learning techniques, VQA methods [25, 26, 41, 51, 61] based on deep neural networks (DNNs) can extract more complex and abstract features related to

video quality and achieve superior performance than traditional methods. However, most deep learning approaches focus on the effect of spatial and temporal video distortion on video quality, without adequately considering the relationship between video quality factors and human feelings. It’s pretty obvious that human judgments are always influenced by subjective feelings, as shown in Fig. 1, two videos with the same quality but different content have different subjective quality scores. Considering that all the current datasets used for VQA are labeled based on HVS, incorporating human feelings into VQA enables the model to achieve better consistency with HVS. Although some recent studies [11, 26, 49, 52] have found that the content of the video affects the human judgment of the video quality, these studies model the effect of the content on subjectivity by extracting higher-level abstract features that are not directly related to human feelings, and thus these features do not effectively reflect human feelings.

However, extracting features related to human feelings from video is challenging due to the lack of research on how video affects human feelings. Recently, Wang et al. [47] revealed that Contrastive Language-Image Pre-training (CLIP) [36] could evaluate the quality of images by using paired antonym prompts and achieved high consistency with human feelings on common IQA datasets [9, 10, 18]. This informs our study, but there are no studies showing that CLIP still has perceptual abilities similar to human feelings in video. Therefore, **an important contribution of this paper is to verify for the first time that CLIP has a high degree of consistency with human feelings in video perception** through extensive experiments, as detailed in Sec. 3. This opens up the possibility of incorporating human feelings into VQA tasks.

Based on the previous study, in this paper, we further propose a novel model to enhance video quality assessment (VQA) by incorporating high-level semantic information related to human feelings (denoted as CLiF-VQA), which further introduces high-level semantic features related to human feelings on top of the low-level-aware features extracted by FAST-VQA [50]. Specifically, we use a set of objective (e.g., bright, blurry, noisy, colorful, etc.) and subjective (e.g., pleasant, boring, fearful, etc.) descriptions that are closely related to human feelings as prompts. Further, we design a semantic feature extractor (SFE) which extracts high-level semantic features corresponding to the descriptions in multiple regions of the video frame. Finally, we fuse the low-level-aware and high-level semantic features to obtain the video quality score.

Our contributions can be summarized as follows:

- **We validate for the first time that CLIP is highly consistent with human feelings in video quality perception.** (Sec. 3)

- **We propose CLiF-VQA, which incorporates for the first time features related to human feelings.** It predicts the quality of a video by fusing high-level semantic features related to human feelings extracted by SEF and low-level perceptual features extracted by FAST-VQA. Extensive experiments demonstrate that CLiF-VQA achieves the best performance on multiple VQA datasets.
- **We design some efficient objective and subjective descriptions that are related to human feelings.** These descriptions are used as prompts for extracting high-level semantic information from the video.
- **We design a zero-shot advanced semantic feature extractor (SFE) based on CLIP.** It extracts semantic features by sliding over multiple regions of a video frame and splices the same semantic features according to their relative positions to obtain semantic feature maps of the video frame. (Sec. 4)

## 2. Related Works

### 2.1. Classical VQA Methods

Classical VQA methods employ handcrafted features to capture specific types of distortions in the video for quality prediction. Early VQA often apply image quality assessment (IQA) algorithms [14, 24, 32, 33, 59, 60] to obtain frame-level features, and then combine with temporal dimension information to obtain video quality scores. For example, V-CORNIA [57] extends the IQA algorithm CORNIA [60] to VQA to obtain frame-level quality scores, and combines these scores through temporal pooling. However, this method does not fully consider the connection between the spatio-temporal information of the video and how they affect the video quality [2, 19, 37, 38]. Natural video statistics (NVS) can take into account both spatio and temporal information, thus it is applied to address the previous problem. V-BLIINDS [38] extracts spatio-temporal statistical features of frame-differences in the video DCT domain and predicts crude frame quality scores using NIQE [33], then trains a linear kernel support vector regression (SVR) [20]. TLVQM [22] considers two levels of features, first computing low complexity features for each frame to extract frame-level statistical features related to motion, and then computing high complexity features related to spatial distortion for representative frames. VIDEVAL [45] applies various handcrafted features to detect and measure the distortions and reduces the computational complexity by reducing the feature dimensions.

### 2.2. Deep Learning-based VQA Methods

Recently, deep learning-based VQA Methods [3, 25, 26, 29, 41, 50–54, 58, 61, 63–65] have gradually achieved bet-

ter performance than classical methods. Rather than relying on handcrafted features, deep VQA methods employ convolutional neural networks (CNN) [12, 13, 15, 16, 39, 42–44] or Transformer models [7, 30, 31] to extract complex and abstract features that are relevant to video quality aspects. For example, VSFA [26] extracts spatial features of video frames using ResNet-50 [15] pre-trained on ImageNet [6], and then models the temporal features using GRU [4]. Similar to the architecture of VSFA, while GST-VQA [3] applies VGG-16 [39] to extract spatial features of videos. To better capture the spatio-temporal information of the video, some works [29, 41, 49, 61–63] adopt 3D-CNN. For example, V-MEON [29] adopts a multi-task framework which utilizes 3D-CNN to extract spatio-temporal features to predict the quality of the video. Other studies [41, 49, 61, 63] combine both 2D-CNN and 3D-CNN to capture the spatial and temporal features of video, and then integrate the two features for quality prediction. Recently, VQA methods [50–52] using the transformer structure have achieved better results relative to CNN. DisCoVQA [52] uses Video Swin Transformer [31] to extract multi-level spatio-temporal features and improves the learning efficiency of the model by temporal sampling of the features. Similarly, FAST-VQA [50] and FasterVQA [51] obtain fragments by spatial-temporal grid mini-cube sampling (St-GMS) and then feed the fragments into a modified Video Swin Transformer [31].

Although deep learning-based VQA methods can extract complex high-level semantic features, these features are not directly related to the human point of view. Two recent works [55, 56] attempt to address this issue. Specifically, MaxVQA [55] captures a variety of quality factors that can be observed by humans through a modified vision-language foundation model CLIP and can jointly evaluate multiple specific quality factors and overall perceptual quality scores. Dover [56] assesses video quality from both aesthetic and technical perspectives by collecting a large number of subjective human quality opinions, so it relatively well models the human process of perceiving quality.

### 3. CLIP for Video Perception

Recently, Wang et al. [47] revealed that CLIP could evaluate the quality of images by using paired antonym prompts and achieved high consistency with human feelings on common IQA datasets [9, 10, 18]. Inspired by their work, we further explore the performance of CLIP in video perception. Unlike the pairwise antonym prompts strategy they used, we apply multiple objective descriptions related to quality factors (e.g., bright, contrast, etc.) and multiple subjective descriptions related to human feelings (e.g., interesting, exciting, etc.) as prompts to obtain features in multiple dimensions of the video corresponding to the descriptions, as shown in Fig. 2. We extract semantic features from multiple regions  $224 \times 224$  with the help of CLIP on all video

frames by means of sliding window. Then we compute the mean of all the feature values corresponding to a specific description as the feature of the video for that description.

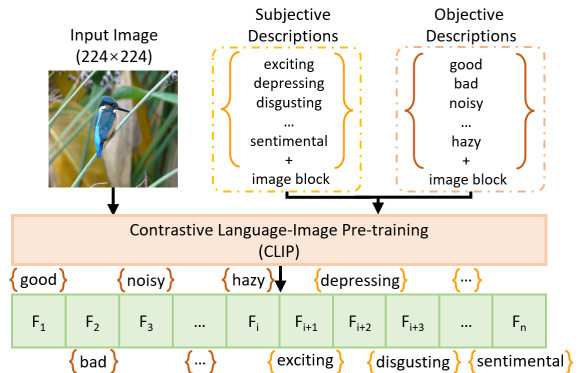


Figure 2. The process of extracting semantic features using CLIP.

Here, we refer to HVS’s perception of video quality factors and content as objective and subjective feelings, respectively. Further, we explore the correlation between CLIP and human objective feelings and subjective feelings.

**Perception of Objective Feelings.** We explore the performance of CLIP on four objective descriptions (bright, contrast, noisy, colorful) related to video quality factors, as shown in Fig. 3. Specifically, we first process the video corresponding to a certain description, and then extract the semantic features that correspond to the description. It can be seen that CLIP is able to accurately perceive changes in video quality factors. This shows that CLIP has a good consistency with human objective feelings in the perception of video quality factors.



Figure 3. CLIP for perception of four objective descriptions (bright, contrast, noisy, colorful) related to video quality factors. "-" represents attenuation and "+" represents enhancement.

**Perception of Subjective Feelings.** Furthermore, we explore the relationship between CLIP and human subjective

feelings in video content perception. In particular, we conduct experiments on four subjective descriptions (interesting, exciting, depressing, fearful) that reflect the subjective feelings that video content brings to humans. As shown in Fig. 4. The results demonstrate that CLIP is highly consistent with human judgments in perceiving video content.

interesting		interesting 0.485 exciting 0.313 depressing 0.052 fearful 0.150		interesting 0.421 exciting 0.281 depressing 0.039 fearful 0.259
	exciting		interesting 0.136 exciting 0.611 depressing 0.018 fearful 0.235	
depressing			interesting 0.159 exciting 0.051 depressing 0.736 fearful 0.054	
	fearful		interesting 0.075 exciting 0.099 depressing 0.045 fearful 0.781	

Figure 4. CLIP for perception of four subjective descriptions (interesting, exciting, depressing, fearful) related to human feelings.

**Performance of CLIP in VQA.** The experiments above demonstrate that CLIP has highly consistent results with humans in perceiving both the quality and content of the video separately. However, it remains to be verified whether CLIP is still effective when both objective and subjective descriptions are used as prompts. Therefore, we conduct further experiments to explore CLIP’s performance in video quality perception when using both objective and subjective descriptions that can reflect human feelings.

Specifically, we use multiple objective and subjective descriptions as prompts for CLIP, as shown in Fig. 2 and then we still use the sliding window approach to extract semantic features on video frames, and finally we concatenate all the semantic features of each frame to obtain the feature vector of each frame of the video. Then we adopt the architecture of the classical VQA model VSFA [26] to input the feature vectors of the frames into the GRU for regression and time pooling operation to get the quality scores. We conduct our experiments on the KoNViD-1k dataset [17], and in addition to processing the comparison with the VSFA model, we also compare with two feature extraction methods (VGG-16 [39] and EfficientNet-V2 [43]) widely used in VQA. And we evaluate performance on SROCC, KROCC and PLCC metrics, as shown in Fig. 5.

The results demonstrate that using both objective and subjective descriptions can achieve better results, compared to using a single description. Furthermore, it can be observed that relying on only features related to human feelings surpasses CNN extracted features in VQA. The exper-

imental results also confirm the prompts of our design.

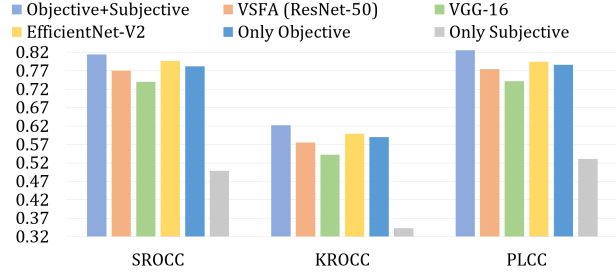


Figure 5. Performance using different descriptions as prompts and comparison results with some classical methods (ResNet-50 [15], VGG-16 [39], EfficientNet-V2 [43]) on KoNViD-1k dataset .

## 4. Approach

In this section, we introduce the proposed CLiF-VQA, which consists of the semantic feature extraction module 4.1 and the spatial feature extraction module 4.2, as shown in Fig. 6. First, we employ the semantic feature extraction module to extract high-level semantic features that are related to human feelings. Then low-level-aware features are extracted using spatial feature extraction module. Finally we fuse these two features through a regression module thus obtaining the video quality score.

### 4.1. Semantic Feature Extraction

In order to effectively extract features that can reflect human feelings, we first design some objective descriptions and subjective descriptions related to human feelings as prompts of CLIP, as shown in Fig. 2. In addition, due to the limitation of the visual coder of CLIP on the input size, we can only extract the semantic information of a small region in the video frame. In order to be able to obtain as much semantic information as possible contained in the video frames, we extracted features from multiple regions of the video frames by sampling them multiple times at different locations, as shown in Fig. 6b. This avoids the loss of video quality caused by resizing and excessive cropping.

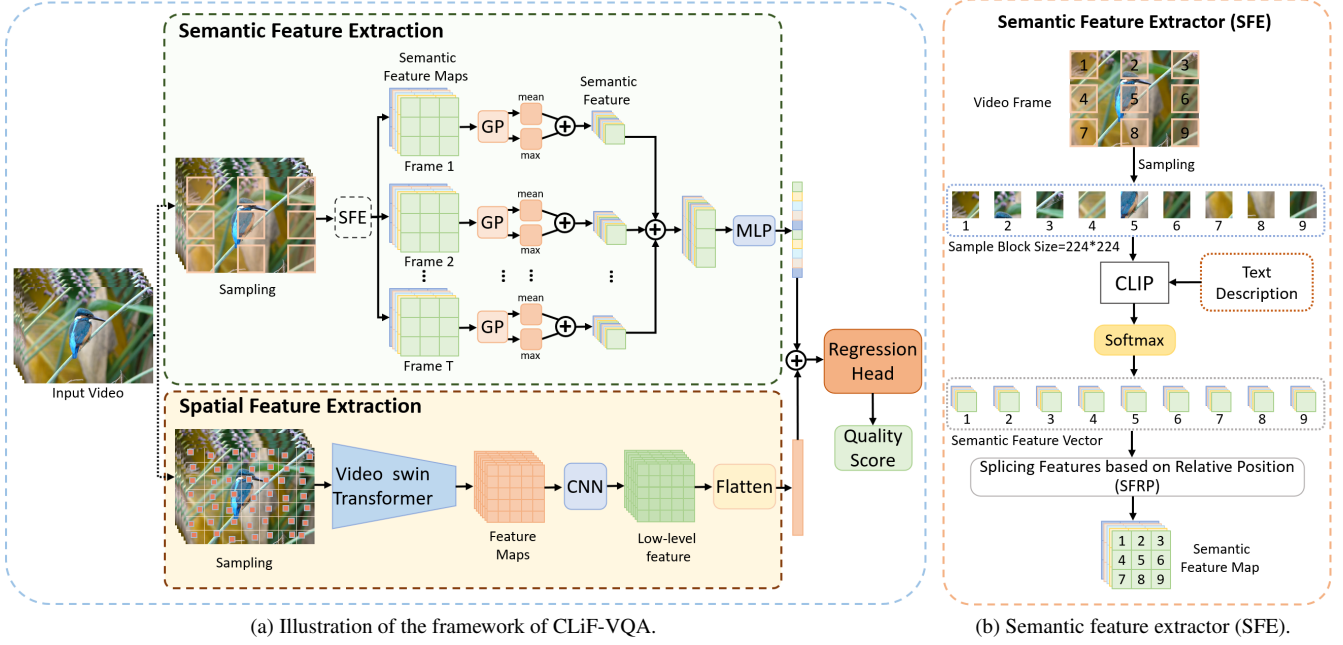
Specifically, assuming the video has  $T$  frames, we perform a sampling operation on the video frames  $I_t (t = 1, 2, \dots, T)$  to obtain  $m \times n$  image blocks of size  $224 \times 224$ :

$$\{b_t^{i,j} | 1 \leq i \leq m, 1 \leq j \leq n\} = \text{Sampling}(I_t) \quad (1)$$

where  $b_t^{i,j}$  represents the block obtained by sampling in the  $i$ -th row and  $j$ -th column.

CLIP calculates the cosine similarity between visual content and descriptions to predict scores for each dimension. We use CLIP to extract high-level semantic features of  $b_t^{i,j}$  related to human feelings. :

$$v_t^{i,j} = \text{Softmax}(\text{CLIP}(b_t^{i,j}), \text{descriptions}) \quad (2)$$



(a) Illustration of the framework of CLiF-VQA.

(b) Semantic feature extractor (SFE).

Figure 6. The framework of our proposed method, which extracts semantic features related to human feelings through the semantic feature extraction module as well as low-level perceptual quality features through a spatial feature extraction module, and then obtains the quality scores by aggregating the two features through the aggregation header.

where descriptions are  $r$  prompts of CLIP, and the feature values of  $v_t^{i,j}$  are the same number and one-to-one correspondence with the number of descriptions.  $Softmax(\cdot)$  is to normalize the output of CLIP.

Then the splicing operation (SFRP) is performed on all the features  $b_t^{i,j}$  based on the relative position to obtain the semantic feature map  $M_t$  of frame  $I_t$ :

$$M_t = SFRP(\{v_t^{i,j} | 1 \leq i \leq m, 1 \leq j \leq n\}) \quad (3)$$

$M_t$  contains  $r$  feature maps, each corresponding to a description. Further, we perform a global average pooling operation ( $GP_{avg}$ ) and a global max pooling operation ( $GP_{max}$ ) on  $M_t$  to obtain the universal features and distinctive features as shown Fig. 6a. The outputs of ( $GP_{avg}$ ) and ( $GP_{max}$ ) are two  $r$ -dimensional feature vectors  $f_t^{avg}$  and  $f_t^{max}$ , respectively.

$$f_t^{avg} = GP_{avg}(M_t) \quad (4)$$

$$f_t^{max} = GP_{max}(M_t) \quad (5)$$

$f_t^{avg}$  and  $f_t^{max}$  are then concatenated as the semantic feature vectors  $f_t$  of the video frame  $I_t$ :

$$f_t = f_t^{avg} \oplus f_t^{max} \quad (6)$$

where  $\oplus$  is the concatenation operator and  $f_t$  is a feature vector of length  $2 \times r$ .

Next, we perform a concatenation operation on the semantic features  $\{f_t\}_{t=1}^T$  of all the video frames thereby obtaining the semantic feature maps  $M_s$  of the video:

$$M_s = f_1 \oplus f_2 \oplus f_3 \oplus \dots \oplus f_T \quad (7)$$

where  $\oplus$  here is not exactly the same as the concatenation of  $\oplus$  in Eq. 6, here  $\oplus$  performs a parallel concatenation on the feature vectors  $\{f_t\}_{t=1}^T$  so that the dimension of the obtained  $M_s$  is  $[2 \times r, T]$ . Each feature map corresponds to a description, and the feature maps here are divided into two types, namely the feature map with global average pooling operation ( $GP_{avg}$ ) and the feature map with global max pooling operation ( $GP_{max}$ ).

After extracting the semantic feature maps of the video, we use a multi-layer perceptron (MLP) to obtain the feature vectors  $F_s$  corresponding to the descriptions. The MLP is composed of two fully connected layers and the activation function is GELU:

$$F_s = FC_2(GELU(FC_1(M_s))) \quad (8)$$

where  $FC_1$  and  $FC_2$  are two fully connected layers and  $F_s$  is a  $2 \times r$  dimensional feature vector.

## 4.2. Spatial Feature Extraction

In VQA, the spatial features of the video play a very important role in estimating the overall video quality. Since low-level information is easily affected by distortion, extracting the low-level-aware features of the video can effectively capture the spatial distortion of the video.

In our approach, we apply FAST-VQA [50] to perceive the low-level quality information in the video. FAST-VQA is a state-of-the-art VQA architecture, which has been proved to be effective in perceiving video distortions and has demonstrated outstanding performance on multiple VQA datasets. Specifically, a new fragments sampling strategy is applied to obtain video fragments  $V_f$ , which preserves the distortion information of the video  $V$  by splicing multiple small patches cropped at the original resolution. Since continuous frame sampling is applied during the sampling process,  $V_f$  preserves the temporal distortion to some extent. The video fragments  $V_f$  are then fed into a modified Video Swin Transformer Tiny [31]:

$$M_f = \text{Transformer}(V_f) \quad (9)$$

Next, the obtained features  $M_f$  are further processed by two 3D convolutional layers to obtain the final feature maps  $M_{final}$  of the video.

$$M_{final} = \text{Conv3D}_2(\text{GELU}(\text{Conv3D}_1(M_f))) \quad (10)$$

Finally we flatten the feature maps  $M_{final}$  to obtain the spatial feature vector  $F_f$  of the video.

$$F_f = \text{Flatten}(M_{final}) \quad (11)$$

In addition, although FAST-VQA can extract effective spatial quality perceptual features in the video, most of the video content is lost due to the segments sampling of FAST-VQA, thus seriously destroying the important information in the video related to human feelings. Therefore, the semantic features related to human feelings extracted in Sec. 4.1 can exactly complement the spatial features extracted by FAST-VQA.

### 4.3. Quality Regression

After extracting the semantic and spatial features of the video through the semantic feature extraction module and spatial feature extraction module, we need to map these features to the quality scores via a regression model. First, We concatenate the semantic features  $F_s$  and spatial features  $F_f$  to get the overall features  $F_v$  of the video:

$$F_v = F_s \oplus F_f \quad (12)$$

Then we design a regression head with two fully connected layers to predict the quality score of the video:

$$\text{Score} = \text{FC}_4(\text{GELU}(\text{FC}_3(F_v))) \quad (13)$$

### 4.4. Loss Function

The loss function used to optimize the proposed models consists of two parts: the monotonicity-induced loss and linearity-induced loss. Given  $m$  predicted quality scores

$\hat{Q} = \{\hat{q}_1, \hat{q}_2, \dots, \hat{q}_m\}$  and  $m$  ground-truth subjective quality scores  $Q = \{q_1, q_2, \dots, q_m\}$ .

Specifically, the monotonicity-induced loss predicts the monotonicity of the video quality scores by introducing additional order constraints. The monotonicity-induced loss function is defined as follows:

$$L_{mon} = \frac{1}{m^2} \sum_{i=1}^m \sum_{j=1}^m \max(0, |q_i - q_j| - f(q_i, q_j) \cdot (\hat{q}_i - \hat{q}_j)) \quad (14)$$

where  $f(q_i, q_j) = 1$  if  $q_i \geq q_j$ , otherwise  $f(q_i, q_j) = -1$ .

In contrast, the goal of the linearity-induced loss is to compute the linear relationship between the predicted quality score and ground-truth subjective quality score. The linearity-induced loss function can be denoted as:

$$\left(1 - \frac{\sum_{i=1}^m (\hat{q}_i - \hat{a})(q_i - a)}{\sqrt{\sum_{i=1}^m (\hat{q}_i - \hat{a})^2 \sum_{i=1}^m (q_i - a)^2}}\right) / 2 \quad (15)$$

where  $a = \frac{1}{m} \sum_{i=1}^m q_i$  and  $\hat{a} = \frac{1}{m} \sum_{i=1}^m \hat{q}_i$ .

Finally, the total loss function  $L$  is obtained by combining the two loss functions  $L_{mon}$  and  $L_{lin}$  above:

$$L = \alpha L_{mon} + \beta L_{lin} \quad (16)$$

where  $\alpha$  and  $\beta$  represent the weights of monotonicity-induced loss and linearity-induced loss.

## 5. Experiments

### 5.1. Experimental Setups

**Datasets.** We test the proposed model on four datasets including LSVQ [61], KoNViD-1k (1200 videos) [17], LIVE-VQC (585 videos) [40], and YouTube-UGC [48]. Specifically, we pre-train CLiF-VQA on LSVQ<sub>train</sub>, a subset of LSVQ containing 28,056 videos.

Intra-dataset testing is performed on two subsets of LSVQ, LSVQ<sub>test</sub> (7400 videos) and LSVQ<sub>1080p</sub> (3600 videos). KoNViD-1k and LIVE-VQC And we perform cross-dataset testing on KoNViD-1k and LIVE-VQC. Further, we fine-tune the model on KoNViD-1k, LIVE-VQC, and YouTube-UGC. It should be noted that YouTube-UGC contains 1500 videos, but only 1147 videos are available to us.

**Evaluation Criteria.** Spearman Rank Order Correlation Coefficient (SROCC) and Pearson Linear Correlation Coefficient (PLCC) are used as evaluation Metrics. Specifically, SRCC is used to measure the prediction monotonicity between predicted scores and true scores by ranking the values in both series and calculating the linear correlation between the two ranked series. In contrast, PLCC evaluates prediction accuracy by calculating the linear correlation between a series of predicted scores and true scores. And higher SROCC and PLCC scores indicate better performance.

Table 1. Experimental performance of the pre-trained CLiF-VQA model on the LSVQ dataset on four test sets (LSVQ<sub>test</sub>, LSVQ<sub>1080p</sub>, KoNViD-1k, LIVE-VQC). LSVQ<sub>test</sub> and LSVQ<sub>1080p</sub> are used for intra-dataset testing. While KoNViD-1k and LIVE-VQC are used for cross-dataset testing. Best in **red** and second in **blue**.

Testing Type		Intra-dataset Test Sets				Cross-dataset Test Sets			
Texting set		LSVQ <sub>test</sub>		LSVQ <sub>1080p</sub>		KoNViD-1k		LIVE-VQC	
Methods	Source	SROCC	PLCC	SROCC	PLCC	SROCC	PLCC	SROCC	PLCC
BRISQUE [32]	TIP, 2012	0.569	0.576	0.497	0.531	0.646	0.647	0.524	0.536
TLVQM [22]	TIP, 2019	0.772	0.774	0.589	0.616	0.732	0.724	0.670	0.691
VIDEVAL [45]	TIP, 2021	0.794	0.783	0.545	0.554	0.751	0.741	0.630	0.640
VSFA [26]	ACMMM, 2019	0.801	0.796	0.675	0.704	0.784	0.794	0.734	0.772
PVQ <sub>w/o/patch</sub> [61]	CVPR, 2021	0.814	0.816	0.686	0.708	0.781	0.781	0.747	0.776
PVQ <sub>w/patch</sub> [61]	CVPR, 2021	0.827	0.828	0.711	0.739	0.791	0.795	0.770	0.807
BVQA [25]	TCSVT, 2022	0.852	0.854	0.771	0.782	0.834	0.837	0.816	0.824
FAST-VQA-M [50]	ECCV, 2022	0.852	0.854	0.739	0.773	0.841	0.832	0.788	0.810
FasterVQA [51]	TPAMI, 2023	0.873	0.874	0.772	0.811	0.863	0.863	0.813	0.837
FAST-VQA [50]	ECCV, 2022	0.872	0.874	0.770	0.809	0.864	0.862	<b>0.824</b>	<b>0.841</b>
DOVER [56]	ICCV, 2023	<b>0.881</b>	<b>0.879</b>	<b>0.782</b>	<b>0.827</b>	<b>0.879</b>	<b>0.885</b>	0.807	<b>0.841</b>
<b>CLiF-VQA</b>	<b>Ours</b>	<b>0.882</b>	<b>0.882</b>	<b>0.788</b>	<b>0.830</b>	<b>0.870</b>	<b>0.866</b>	<b>0.835</b>	<b>0.856</b>

**Implementation Details.** we employ PyTorch framework and an NVIDIA GeForce RTX 3090 card to train the model in all experimental implementations. In the semantic feature extraction module, we sample each frame of the video 9 times and then perform zero-shot feature extraction with CLIP, as shown in Fig. 6b. In the spatial feature extraction module, we employ the FAST-VQA [50] architecture with the Video Swin Transformer Tiny [31] backbone pre-trained on the Kinetics-400 [21] dataset. During training, the initial learning rate of FAST-VQA backbone is set to 0.000075, and the initial learning of other parts is set to 0.00075. We set the batch size to 12 and use the AdamW optimizer with a weight decay rate of 0.05.

## 5.2. Pre-training Results on LSVQ

We pre-train CLiF-VQA on the LSVQ dataset and compare it with the existing advanced classical and deep VQA methods on four test sets, as shown in Tab. 1. All experiments are conducted under 10 train-test splits. Compared with some classical methods (BRISQUE, TLVQM, VIDEVAL), CLiF-VQA achieves a significant improvement in performance on all test sets. In addition, CLiF-VQA gives better results on all test sets compared to FAST-VQA, which focuses only on low-level-aware features of the video. This suggests that the introduced human perception features can well complement the features extracted by FAST-VQA, thus improving the prediction accuracy of the model. Furthermore, CLiF-VQA has improved performance on the intra-dataset test sets compared to the current state-of-the-art DOVER (our reproduced). And CLiF-VQA also significantly outperforms the best results on LIVE-VQA in the cross-dataset test.

## 5.3. Fine-tuning Results on Small Datasets

In Tab. 2, we fine-tune CLiF-VQA on three small datasets (LIVE-VQC, KoNViD-1k, YouTube-UGC). As before, all experiments are conducted under 10 train-test splits. Here, we further test the results of CLiF-VQA fine-tuning on small data sets, when pre-training only the FAST-VQA branch on LSVQ. It can be seen that CLiF-VQA\* performs better than FAST-VQA on all three datasets. It even surpasses DOVER on the LIVE-VQC dataset. In addition, CLiF-VQA pretrained on LSVQ outperforms the current state-of-the-art DOVER (our reproduced) on all three datasets.

## 5.4. Ablation Studies

**Ablation on the Compositions of CLiF-VQA.** We validate the effectiveness of the three modules that make up CLiF-VQA. As shown in Tab. 3, CLiF-VQA has acceptable performance when only semantic features related to human feelings are extracted, and the performance of CLiF-VQA is further improved when the regression head module is introduced. However, when only low-level perceptual features of the video are extracted using FAST-VQA, there is no significant improvement in performance after the introduction of the regression head. When both branches are considered simultaneously, the performance of the model improves significantly relative to the use of a single branch and is further improved with the introduction of the regression header.

**Ablation on Descriptions.** In Tab. 4, we verify the effect of different types of descriptions on the performance of CLiF-VQA. The results demonstrate that objective descriptions have a greater impact on the performance improvement of CLiF-VQA compared to subjective descriptions. And the optimal results can be obtained by using both objective and

Table 2. The finetune results on LIVE-VQC, KoNViD and YouTube-UGC datasets. CLiF-VQA\* indicates that only the FAST-VQA branch is pre-trained on LSVQ, instead of training the whole model. CLiF-VQA\* pre-trained only the spatial feature extraction branch on LSVQ. Best in **red** and second in **blue**.

Finetune Datasets		LIVE-VQC		KoNViD-1k		YouTube-UGC	
Methods	Source	SROCC	PLCC	SROCC	PLCC	SROCC	PLCC
TLVQM [22]	TIP, 2019	0.799	0.803	0.773	0.768	0.669	0.659
VIDEVAL [45]	TIP, 2021	0.752	0.751	0.783	0.780	0.779	0.773
RAPIQUE [46]	OJSP, 2021	0.755	0.786	0.803	0.817	0.759	0.768
CNN+TLVQM [23]	ACMMM, 2020	0.825	0.834	0.816	0.818	0.809	0.802
CNN+VIDEVAL [45]	TIP, 2021	0.785	0.810	0.815	0.817	0.808	0.803
VSFA [26]	ACMMM, 2019	0.773	0.795	0.773	0.775	0.724	0.743
PVQ [61]	CVPR, 2021	0.827	0.837	0.791	0.786	NA	NA
GST-VQA [3]	TCSVT, 2021	NA	NA	0.814	0.825	NA	NA
CoINVQ [49]	TCSVT, 2021	NA	NA	0.767	0.764	0.816	0.802
BVQA [25]	TCSVT, 2022	0.831	0.842	0.834	0.836	0.831	0.819
FAST-VQA-M [50]	ECCV, 2022	0.803	0.828	0.873	0.872	0.768	0.765
FasterVQA [51]	TPAMI, 2023	0.843	0.858	0.895	0.898	0.863	0.859
FAST-VQA [50]	ECCV, 2022	0.845	0.852	0.890	0.889	0.857	0.853
DOVER [56]	ICCV, 2023	0.812	0.852	<b>0.897</b>	<b>0.899</b>	<b>0.879</b>	<b>0.883</b>
<b>CLiF-VQA*</b>	<b>Ours</b>	<b>0.856</b>	<b>0.860</b>	0.894	0.895	0.868	0.870
<b>CLiF-VQA</b>	<b>Ours</b>	<b>0.864</b>	<b>0.880</b>	<b>0.902</b>	<b>0.903</b>	<b>0.888</b>	<b>0.891</b>

Table 3. Ablation study of three main components: Semantic (Semantic Feature Extraction Module), Spatial (Spatial Feature Extraction Module) and Regression (Regression Head). SROCC and PLCC are the average results over the three datasets (LIVE-VQC, KoNViD-1k, YouTube-UGC).

Semantic	Spatial	Regression	SROCC	PLCC
✓			0.792	0.788
	✓		0.864	0.865
✓		✓	0.812	0.820
	✓	✓	0.868	0.869
✓	✓		0.879	0.882
✓	✓	✓	0.885	0.889

Table 4. Ablation study on descriptions. Obj and Sub denote objective descriptions and subjective descriptions, respectively.

Datasets	LIVE-VQC	KoNViD-1k	YouTube-UGC
Descriptions	SROCC/PLCC	SROCC/PLCC	SROCC/PLCC
None	0.845/0.852	0.890/0.889	0.857/0.853
Only-Obj	0.857/0.868	0.898/0.895	0.880/0.876
Only-Sub	0.849/0.856	0.893/0.891	0.863/0.860
Obj+Sub	0.864/0.873	0.902/0.903	0.888/0.891

subjective descriptions.

**Ablation on the Number of Samples.** We use CLiF-VQA pre-trained on LSVQ for cross-dataset testing. We divide LIVE-VQC into three groups according to the resolution of the videos: 1080p (110 videos), 720p (316 videos), and 540p (159 videos). We then evaluated the performance on these three resolution groups with different numbers of samples (Fig. 6b). As shown in Tab. 5, CLiF-VQA achieves optimal performance with a smaller number of feature extrac-

Table 5. Experimental performance regarding the number of samples taken by the semantic feature extractor on video frames of different resolutions. Videos in all resolutions are from LIVE-VQC.

Resolution	≤540p	720p	1080p
Times	SROCC/PLCC	SROCC/PLCC	SROCC/PLCC
1	0.841/0.876	0.811/0.823	0.812/0.809
5	0.856/0.884	0.825/0.840	0.820/0.822
9	0.862/0.889	0.843/0.858	0.834/0.836
25	<b>0.866/0.890</b>	0.852/0.866	0.847/0.858
45	0.864/0.889	<b>0.855/0.868</b>	0.855/0.867
85	0.864/0.887	0.851/0.862	<b>0.857/0.871</b>

tions on low-resolution videos, while more feature extractions are required for high-resolution videos. It also shows that the 9 times feature extraction performed in this paper does not show the optimal performance of CLiF-VQA. Therefore, the performance of CLiF-VQA proposed in this paper can be further improved by increasing the number of samples.

## 6. Conclusions

In this paper, we first analyze that human subjective feelings have an important impact on video quality evaluation. Further, we verify for the first time the correlation between CLIP and human feelings in video perception. Extensive subjective experiments demonstrate that CLIP not only has good consistency with human feelings, but also can achieve satisfactory results in VQA by using only the features related to human feelings extracted by CLIP. Motivated by these findings, we propose CLiF-VQA, a method that extracts features related to human feelings and low-level



perceptual features of videos. Then, it fuses the two features to obtain the video quality score. Extensive experimental results demonstrate that the proposed CLiF-VQA outperforms existing methods on multiple VQA datasets.

## References

- [1] Mehdi Banitalebi-Dehkordi, Abbas Ebrahimi-Moghadam, Morteza Khademi, and Hadi Hadizadeh. No-reference video quality assessment based on visual memory modeling. *IEEE Trans. Broadcast.*, 66(3):676–689, 2019. [1](#)
- [2] Yoram S Bonneh, Alexander Cooperman, and Dov Sagi. Motion-induced blindness in normal observers. *Nature*, 411(6839):798–801, 2001. [2](#)
- [3] Baoliang Chen, Lingyu Zhu, Guo Li, Fangbo Lu, Hongfei Fan, and Shiqi Wang. Learning generalized spatial-temporal deep feature representation for no-reference video quality assessment. *IEEE TCSVT*, 32(4):1903–1916, 2021. [2](#), [3](#), [8](#)
- [4] Kyunghyun Cho, Bart Van Merriënboer, Caglar Gulcehre, Dzmitry Bahdanau, Fethi Bougares, Holger Schwenk, and Yoshua Bengio. Learning phrase representations using rnn encoder-decoder for statistical machine translation. *arXiv preprint arXiv:1406.1078*, 2014. [3](#)
- [5] Sathya Veera Reddy Dendi and Sumohana S Channappayya. No-reference video quality assessment using natural spatiotemporal scene statistics. *IEEE TIP*, 29:5612–5624, 2020. [1](#)
- [6] Jia Deng, Wei Dong, Richard Socher, Li-Jia Li, Kai Li, and Li Fei-Fei. Imagenet: A large-scale hierarchical image database. In *CVPR*, pages 248–255. IEEE, 2009. [3](#)
- [7] Alexey Dosovitskiy, Lucas Beyer, Alexander Kolesnikov, Dirk Weissenborn, Xiaohua Zhai, Thomas Unterthiner, Mostafa Dehghani, Matthias Minderer, Georg Heigold, Sylvain Gelly, et al. An image is worth 16x16 words: Transformers for image recognition at scale. *arXiv preprint arXiv:2010.11929*, 2020. [3](#)
- [8] Joshua Peter Ebenezer, Zaixi Shang, Yongjun Wu, Hai Wei, Sriram Sethuraman, and Alan C Bovik. Chipqa: No-reference video quality prediction via space-time chips. *IEEE TIP*, 30:8059–8074, 2021. [1](#)
- [9] Yuming Fang, Hanwei Zhu, Yan Zeng, Kede Ma, and Zhou Wang. Perceptual quality assessment of smartphone photography. In *CVPR*, pages 3677–3686, 2020. [2](#), [3](#)
- [10] Deepti Ghadiyaram and Alan C Bovik. Massive online crowdsourced study of subjective and objective picture quality. *IEEE TIP*, 25(1):372–387, 2015. [2](#), [3](#)
- [11] Franz Götz-Hahn, Vlad Hosu, Hanhe Lin, and Dietmar Saupe. Konvid-150k: A dataset for no-reference video quality assessment of videos in-the-wild. *IEEE Access*, 9:72139–72160, 2021. [2](#)
- [12] Kensho Hara, Hirokatsu Kataoka, and Yutaka Satoh. Learning spatio-temporal features with 3d residual networks for action recognition. In *ICCV Workshops*, pages 3154–3160, 2017. [3](#)
- [13] Kensho Hara, Hirokatsu Kataoka, and Yutaka Satoh. Can spatiotemporal 3d cnns retrace the history of 2d cnns and imagenet? In *CVPR*, pages 6546–6555, 2018. [3](#)
- [14] Rania Hassen, Zhou Wang, and Magdy MA Salama. Image sharpness assessment based on local phase coherence. *IEEE TIP*, 22(7):2798–2810, 2013. [2](#)
- [15] Kaiming He, Xiangyu Zhang, Shaoqing Ren, and Jian Sun. Deep residual learning for image recognition. In *CVPR*, pages 770–778, 2016. [3](#), [4](#)
- [16] Kaiming He, Xiangyu Zhang, Shaoqing Ren, and Jian Sun. Identity mappings in deep residual networks. In *ECCV*, pages 630–645. Springer, 2016. [3](#)
- [17] Vlad Hosu, Franz Hahn, Mohsen Jenadeleh, Hanhe Lin, Hui Men, Tamás Szirányi, Shujun Li, and Dietmar Saupe. The konstanz natural video database (konvid-1k). In *QoMEX*, pages 1–6. IEEE, 2017. [1](#), [4](#), [6](#)
- [18] Vlad Hosu, Hanhe Lin, Tamas Sziranyi, and Dietmar Saupe. Koniq-10k: An ecologically valid database for deep learning of blind image quality assessment. *IEEE TIP*, 29:4041–4056, 2020. [2](#), [3](#)
- [19] Quan Huynh-Thu and Mohammed Ghanbari. Temporal aspect of perceived quality in mobile video broadcasting. *IEEE Trans. on Broadcast.*, 54(3):641–651, 2008. [2](#)
- [20] Alexandros Karatzoglou, Alexandros Smola, Kurt Hornik, and Achim Zeileis. kernlab-an s4 package for kernel methods in r. *Journal of Statistical Software*, 11:1–20, 2004. [2](#)
- [21] Will Kay, Joao Carreira, Karen Simonyan, Brian Zhang, Chloe Hillier, Sudheendra Vijayanarasimhan, Fabio Viola, Tim Green, Trevor Back, Paul Natsev, et al. The kinetics human action video dataset. *arXiv preprint arXiv:1705.06950*, 2017. [7](#)
- [22] Jari Korhonen. Two-level approach for no-reference consumer video quality assessment. *IEEE TIP*, 28(12):5923–5938, 2019. [1](#), [2](#), [7](#), [8](#)
- [23] Jari Korhonen, Yicheng Su, and Junyong You. Blind natural video quality prediction via statistical temporal features and deep spatial features. In *ACM MM*, pages 3311–3319, 2020. [8](#)
- [24] Debarati Kundu, Deepti Ghadiyaram, Alan C Bovik, and Brian L Evans. No-reference quality assessment of tone-mapped hdr pictures. *IEEE TIP*, 26(6):2957–2971, 2017. [2](#)
- [25] Bowen Li, Weixia Zhang, Meng Tian, Guangtao Zhai, and Xianpei Wang. Blindly assess quality of in-the-wild videos via quality-aware pre-training and motion perception. *IEEE TCSVT*, 32(9):5944–5958, 2022. [1](#), [2](#), [7](#), [8](#)
- [26] Dingquan Li, Tingting Jiang, and Ming Jiang. Quality assessment of in-the-wild videos. In *ACM MM*, pages 2351–2359, 2019. [1](#), [2](#), [3](#), [4](#), [7](#), [8](#)
- [27] Yang Li, Shengbin Meng, Xinfeng Zhang, Shiqi Wang, Yue Wang, and Siwei Ma. Ugc-video: perceptual quality assessment of user-generated videos. In *MIPR*, pages 35–38. IEEE, 2020. [1](#)
- [28] Liang Liao, Kangmin Xu, Haoning Wu, Chaofeng Chen, Wenxiu Sun, Qiong Yan, and Weisi Lin. Exploring the effectiveness of video perceptual representation in blind video quality assessment. In *ACM MM*, pages 837–846, 2022. [1](#)
- [29] Wentao Liu, Zhengfang Duanmu, and Zhou Wang. End-to-end blind quality assessment of compressed videos using deep neural networks. In *ACM MM*, pages 546–554, 2018. [2](#), [3](#)

- [30] Ze Liu, Yutong Lin, Yue Cao, Han Hu, Yixuan Wei, Zheng Zhang, Stephen Lin, and Baining Guo. Swin transformer: Hierarchical vision transformer using shifted windows. In *ICCV*, pages 10012–10022, 2021. 3
- [31] Ze Liu, Jia Ning, Yue Cao, Yixuan Wei, Zheng Zhang, Stephen Lin, and Han Hu. Video swin transformer. In *CVPR*, pages 3202–3211, 2022. 3, 6, 7
- [32] Anish Mittal, Anush Krishna Moorthy, and Alan Conrad Bovik. No-reference image quality assessment in the spatial domain. *IEEE TIP*, 21(12):4695–4708, 2012. 2, 7
- [33] Anish Mittal, Rajiv Soundararajan, and Alan C Bovik. Making a “completely blind” image quality analyzer. *IEEE SPL*, 20(3):209–212, 2012. 2
- [34] Anish Mittal, Michele A Saad, and Alan C Bovik. A completely blind video integrity oracle. *IEEE TIP*, 25(1):289–300, 2015. 1
- [35] Mikko Nuutinen, Toni Virtanen, Mikko Vaahteranoksa, Tero Vuori, Pirkko Oittinen, and Jukka Häkkinen. CVD2014—A database for evaluating no-reference video quality assessment algorithms. *IEEE TIP*, 25(7):3073–3086, 2016. 1
- [36] Alec Radford, Jong Wook Kim, Chris Hallacy, Aditya Ramesh, Gabriel Goh, Sandhini Agarwal, Girish Sastry, Amanda Askell, Pamela Mishkin, Jack Clark, et al. Learning transferable visual models from natural language supervision. In *ICML*, pages 8748–8763. PMLR, 2021. 2
- [37] John G Robson. Spatial and temporal contrast-sensitivity functions of the visual system. *Josa*, 56(8):1141–1142, 1966. 2
- [38] Michele A Saad, Alan C Bovik, and Christophe Charrier. Blind prediction of natural video quality. *IEEE TIP*, 23(3):1352–1365, 2014. 1, 2
- [39] Karen Simonyan and Andrew Zisserman. Very deep convolutional networks for large-scale image recognition. *arXiv preprint arXiv:1409.1556*, 2014. 3, 4
- [40] Zeina Sinno and Alan Conrad Bovik. Large-scale study of perceptual video quality. *IEEE TIP*, 28(2):612–627, 2018. 1, 6
- [41] Wei Sun, Xionghuo Min, Wei Lu, and Guangtao Zhai. A deep learning based no-reference quality assessment model for ugc videos. In *ACM MM*, pages 856–865, 2022. 1, 2, 3
- [42] Mingxing Tan and Quoc Le. Efficientnet: Rethinking model scaling for convolutional neural networks. In *ICML*, pages 6105–6114. PMLR, 2019. 3
- [43] Mingxing Tan and Quoc Le. Efficientnetv2: Smaller models and faster training. In *ICML*, pages 10096–10106. PMLR, 2021. 4
- [44] Du Tran, Lubomir Bourdev, Rob Fergus, Lorenzo Torresani, and Manohar Paluri. Learning spatiotemporal features with 3d convolutional networks. In *ICCV*, pages 4489–4497, 2015. 3
- [45] Zhengzhong Tu, Yilin Wang, Neil Birkbeck, Balu Adsumilli, and Alan C Bovik. UGC-VQA: benchmarking blind video quality assessment for user generated content. *IEEE TIP*, 30:4449–4464, 2021. 1, 2, 7, 8
- [46] Zhengzhong Tu, Xiangxu Yu, Yilin Wang, Neil Birkbeck, Balu Adsumilli, and Alan C Bovik. Rapique: Rapid and accurate video quality prediction of user generated content. *IEEE OJSP*, 2:425–440, 2021. 8
- [47] Jianyi Wang, Kelvin CK Chan, and Chen Change Loy. Exploring clip for assessing the look and feel of images. In *AAAI*, pages 2555–2563, 2023. 2, 3
- [48] Yilin Wang, Sasi Inguva, and Balu Adsumilli. Youtube ugc dataset for video compression research. In *MMSP*, pages 1–5. IEEE, 2019. 1, 6
- [49] Yilin Wang, Junjie Ke, Hossein Talebi, Joong Gon Yim, Neil Birkbeck, Balu Adsumilli, Peyman Milanfar, and Feng Yang. Rich features for perceptual quality assessment of ugc videos. In *CVPR*, pages 13435–13444, 2021. 2, 3, 8
- [50] Haoning Wu, Chaofeng Chen, Jingwen Hou, Liang Liao, Annan Wang, Wenxiu Sun, Qiong Yan, and Weisi Lin. Fastvqa: Efficient end-to-end video quality assessment with fragment sampling. In *ECCV*, pages 538–554. Springer, 2022. 2, 3, 6, 7, 8
- [51] Haoning Wu, Chaofeng Chen, Liang Liao, Jingwen Hou, Wenxiu Sun, Qiong Yan, Jinwei Gu, and Weisi Lin. Neighbourhood representative sampling for efficient end-to-end video quality assessment. *IEEE TPAMI*, 2023. 1, 3, 7, 8
- [52] Haoning Wu, Chaofeng Chen, Liang Liao, Jingwen Hou, Wenxiu Sun, Qiong Yan, and Weisi Lin. Discovqa: Temporal distortion-content transformers for video quality assessment. *IEEE TCSVT*, 2023. 2, 3
- [53] Haoning Wu, Liang Liao, Jingwen Hou, Chaofeng Chen, Erli Zhang, Annan Wang, Wenxiu Sun, Qiong Yan, and Weisi Lin. Exploring opinion-unaware video quality assessment with semantic affinity criterion. *ICME*, 2023.
- [54] Haoning Wu, Liang Liao, Annan Wang, Chaofeng Chen, Jingwen Hou, Wenxiu Sun, Qiong Yan, and Weisi Lin. Towards robust text-prompted semantic criterion for in-the-wild video quality assessment. *arXiv preprint arXiv:2304.14672*, 2023. 2
- [55] Haoning Wu, Erli Zhang, Liang Liao, Chaofeng Chen, Jingwen Hou, Annan Wang, Wenxiu Sun, Qiong Yan, and Weisi Lin. Towards explainable in-the-wild video quality assessment: A database and a language-prompted approach. In *ACM MM*, page 1045–1054, 2023. 3
- [56] Haoning Wu, Erli Zhang, Liang Liao, Chaofeng Chen, Jingwen Hou, Annan Wang, Wenxiu Sun, Qiong Yan, and Weisi Lin. Exploring video quality assessment on user generated contents from aesthetic and technical perspectives. In *ICCV*, pages 20144–20154, 2023. 3, 7, 8
- [57] Jingtao Xu, Peng Ye, Yong Liu, and David Doermann. No-reference video quality assessment via feature learning. In *ICIP*, pages 491–495. IEEE, 2014. 2
- [58] Jiahua Xu, Jing Li, Xingguang Zhou, Wei Zhou, Baichao Wang, and Zhibo Chen. Perceptual quality assessment of internet videos. In *ACM MM*, pages 1248–1257, 2021. 2
- [59] Wufeng Xue, Xuanqin Mou, Lei Zhang, Alan C Bovik, and Xiangchu Feng. Blind image quality assessment using joint statistics of gradient magnitude and laplacian features. *IEEE TIP*, 23(11):4850–4862, 2014. 2
- [60] Peng Ye, Jayant Kumar, Le Kang, and David Doermann. Un-supervised feature learning framework for no-reference image quality assessment. In *CVPR*, pages 1098–1105. IEEE, 2012. 2
- [61] Zhenqiang Ying, Maniratnam Mandal, Deepti Ghadiyaram, and Alan Bovik. Patch-vq: patching up the video quality

- problem. In *CVPR*, pages 14019–14029, 2021. 1, 2, 3, 6, 7, 8
- [62] Junyong You and Jari Korhonen. Deep neural networks for no-reference video quality assessment. In *ICIP*, pages 2349–2353. IEEE, 2019.
- [63] Zicheng Zhang, Wei Wu, Wei Sun, Danyang Tu, Wei Lu, Xionghuo Min, Ying Chen, and Guangtao Zhai. Md-vqa: Multi-dimensional quality assessment for ugc live videos. In *CVPR*, pages 1746–1755, 2023. 2, 3
- [64] Kai Zhao, Kun Yuan, Ming Sun, and Xing Wen. Zoom-vqa: Patches, frames and clips integration for video quality assessment. In *CVPR*, pages 1302–1310, 2023.
- [65] Hanwei Zhu, Baoliang Chen, Lingyu Zhu, and Shiqi Wang. Learning spatiotemporal interactions for user-generated video quality assessment. *IEEE TCSVT*, 33(3): 1031–1042, 2022. 2